# Experimental study on the behavior of CFT stub columns filled with PCC subject to concentric compressive loads

Hyun-Sik Kang† and Seo-Hyung Lim‡

*Department of Architecture, Jinju National University, Korea*

Tae-Sup Moon‡†

*Department of Architectural Engineering, Hanyang University, Seoul, Korea*

S. F. Stiemer‡‡

*Department of Civil Engineering, University of British Columbia, 2324 Main Mall, Vancouver, B.C., Canada, V6T 1Z4*

**Abstract.** This paper presents an experimental study and its findings of the behavior of circular and square stub columns filled with high strength concrete ($f_c'$=49 MPa) and polymer cement concrete (PCC) under concentric compressive load. Twenty-four specimens were tested to investigate the effects of variations in the tube shape (circular, square), wall thickness, and concrete type on the axial strength of stub columns. The characteristics of CFT stub columns filled with two types of concrete were investigated in order to collect the basic design data for using the PCC for the CFT columns. The experimental investigations included consideration of the effects of the concrete fill on the failure mode, ultimate strength, initial stiffness and deformation capacity. One of the key findings of this study was that circular section members filled with PCC retain their structural resistance without reduction far beyond the ultimate capacity. The results presented in this paper will provide experimental data to aid in the development of design procedures for the use of advanced concretes in CFT columns. Additionally, these results give structural designers invaluable insight into the realistic behavior of CFT columns.

**Key words:** polymer cement concrete; CFT stub columns; ultimate strength; failure mode; width-thickness ratio.

## 1. Introduction

The number of high-rise buildings constructed using CFT members has continuously increased since their introduction in the 1960's. In the last decade, Asian countries have experienced a surge in the popularity of CFT members due to their superior structural performance and efficiency, and the

†Assistant Professor (on post-doctoral leave at the University of British Columbia)
‡Assistant Professor
‡†Professor
‡‡Professor, Corresponding author, E-mail: sigi@civil.ubc.ca

increased availability of hollow structural steel sections. A major advantage of using CFT steel tube members is that no formwork is required, resulting in economical construction. The interaction between the concrete core and steel tube has been investigated by Furlong (1968) and Knowles and Park (1969). These characteristics have been previously mentioned by Dunberry *et al.* (1987). Prion and Baraka (1994) who specifically addressed the beam-column behavior of steel tubes filled with high strength concrete. The development of a polynomial equation to represent the three-dimensional (3D) cross-section strength of square or rectangular concrete-filled steel tube (CFT) beam-columns is done by Hajjar and Gourley in 1996. Stephen P. Schneider (1998) tested 14 CFT specimens with circular, square, and rectangular steel tube shapes. *D/t* ratios of the specimens ranged from 17 to 50 and the length-to-tube depth ratios of 4<*L/D*<5 were investigated. Campione *et al.* (2000) evaluated the strength of hollow circular steel sections filled with nominal-strength plain concrete and fiber-reinforced concrete (FRC). The behavior and strength of concrete-filled tube columns under seismic loads was studied by testing six columns, which were subjected to a constant axial load (Elremaily and Azizinamini 2002). Campione and Scibilia (2002) suggested a simplified expression for the calculation of the load-deflection curves for short tubular steel columns filled with concrete based on experimental and theoretical results. Huang *et al.* (2002). investigated the axial load behavior of CFT columns with width-to-thickness ratios ranging from 40 to 150. Results suggested that current specifications might considerably underestimate the ultimate load of circular CFT columns. Han investigated the behavior of stub columns with rectangular hollow sections filled with concrete subjected to axial load. Bradford *et al.* carried out an analysis to determine a crossed form solution for the elastic buckling of circular tube with a rigid infill in 2002. Han *et al.* investigated the behavior of concrete-filled steel square hollow section (SHS) and rectangular hollow section (RHS) columns with and without fire protection subjected to axial loads in 2003. Zhao *et al.* (2004) developed a mechanical model for concrete-filled steel circular hollow section (CHS) beam-columns.

Though many design codes deal with CFT members, there is a lack of consistency between codes. In Korea, the basic document for the field was published in 2001, entitled Recommendations for the Design and Construction of CFT Structures, and is based on allowable stress design. However, the design strength of concrete specified by the document was limited to less than 49 Mpa, and it was recommended that CFT columns using concrete strengths above this value should be evaluated experimentally. This paper therefore focuses on the behavior of CFT stub columns filled with high strength normal concrete and polymer cement concrete (PCC). Load carrying capacity, failure mode, initial stiffness, and load-strain relationships were recorded. Test results were compared with calculated values following the AISC (1994), CISC (1997), KSSC (2001), and EC4 (1994) codes.

## 2. Experimental procedure

### 2.1. *Test specimen parameters*

The main experimental parameters are listed below, along with the labels used to characterize each specimen:
- Section shape (C=circular tube, S=square tube)
- Concrete fill type (E=empty, F=normal concrete, P=PCC)
- Polymer mixing rate (0=0%, 2=2%)

For example, specimens beginning with the label "CF0" would be circular columns filled with normal concrete. The width-thickness ratios of the specimens ranged from 13 to 46. The circular sections consisted of SPS400 steel, and the square sections consisted of SPSR400 steel.

## 2.2. Tensile test of steel coupon

Table 1 lists the dimensions and test results for each of the specimens used in the tensile coupon test. Three coupons were cut from the eight types of tubes according to the Standard KSB 0801. The thickness and width of specimens were measured by digital vernier calipers prior to testing, and the flat plates were marked to measure elongation. Uniaxial tensile force was applied using the 1000 kN universal testing machine according to the Standard KSB 0802. The yield ratio of mild structural steel is usually in the range of 0.6 to 0.7, while the test results show higher values in the range of 0.7 to 0.85. The results also show that the elongation of square section steel tubes is typically lower than that of the circular steel tubes. For those cases where the yield point could not clearly be detected, it was determined by using the 0.2% offset method.

## 2.3. Concrete cylinder test

The design mixing strength for the normal concrete was 49 MPa, and the mix proportion per cubic meter of concrete is given in Table 2. As shown in Table 3, the resulting 28-day cylinder strength was 53 MPa for normal concrete and was approximately 46 MPa for PCC. Test cylinders of 100 mm
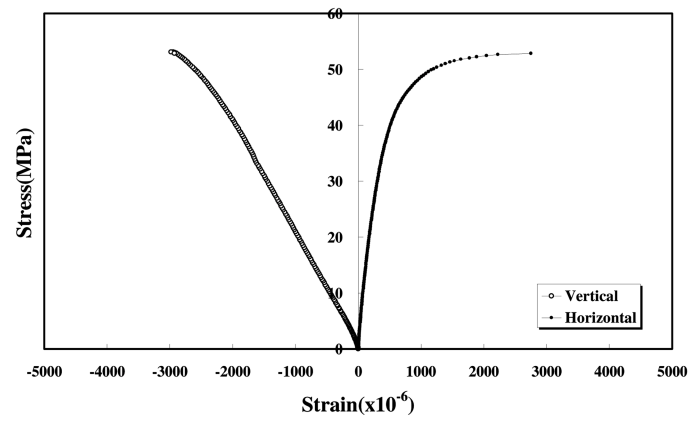
Table 1 Test results of steel coupon

| Specimen type | $\sigma_y$ (MPa) yield stress | $\sigma_{max}$ (MPa) tensile strength | $\varepsilon_y$ ($\times 10^{-6}$) yield strain | $\varepsilon_{max}$ ($\times 10^{-6}$) maximum strain | Lo. (%) elongation | $Y$ ($\sigma_y/\sigma_{max}$) yield ratio |
|---|---|---|---|---|---|---|
| CT-1 | 336 | 394 | 1734 | 46124 | 31.67 | 0.85 |
| CT-2 | 274 | 358 | 3450 | 57810 | 38.30 | 0.77 |
| CT-3 | 271 | 340 | 1777 | 95741 | 33.30 | 0.80 |
| CT-4 | 358 | 423 | 2303 | 79264 | 32.50 | 0.84 |
| ST-1 | 313 | 367 | 2757 | 73030 | 22.10 | 0.85 |
| ST-2 | 372 | 433 | 2498 | 66352 | 16.25 | 0.85 |
| ST-3 | 338 | 462 | 3562 | 60000 | 26.25 | 0.73 |
| ST-4 | 284 | 408 | 3500 | 1382231 | 19.60 | 0.70 |

Table 2 Concrete mix designs

| Material | Quantity (unit weight) | |
|---|---|---|
| | Normal concrete | PCC (polymer cement concrete) |
| Coarse | 815 kg | 848 kg |
| Medium sand | 848 kg | 723 kg |
| Portland cement | 480 kg | 450 kg |
| Polymer | 0 kg | 90 kg |
| Water | 163 kg | 126 kg |
| Water/cement ratio | 34% | 28% |

Table 3 Test results of concrete cylinder

| Remarks | Normal concrete | PCC (polymer cement concrete) |
|---|---|---|
| Compressive strength | 53 MPa | 46 MPa |
| Tensile strength | 3.7 MPa | 3.9 MPa |
| Maximum strain ($\times 10^{-6}$) | 2794 | 4393 |
| Elastic modulus | 2117 MPa | 1519 MPa |



(a) Normal concrete



(b) Polymer cement concrete

Fig. 1 Stress-strain relationship of concrete

diameter, and 200 mm height were used for compressive strength tests according to the Standard KSF 2403. Fig. 1 shows the resulting stress-strain relationship of these specimens.

## 2.4. Stub column test setup

The length of the stub column specimen was chosen to be three times the width. A concentric compressive load was applied to the stub columns by a 2000 kN universal testing machine. Strain was measured by wire strain gauges in the vertical and horizontal directions. Axial displacements were measured by 50 mm linear

Table 4 Test results of stub columns

|  | Name | $P_y$ (KN) | $\delta_y$ (mm) | $P_{max}$ (KN) | $\delta_{max}$ (mm) | Failure mode |
|---|---|---|---|---|---|---|
| Hollow section | CE05-1 | 423 | 1.10 | 463 | 8.19 | 1 |
|  | CE05-2 | 142 | 1.04 | 157 | 3.26 | 1 |
|  | CE05-3 | 198 | 1.21 | 215 | 4.02 | 1 |
|  | CE05-4 | 295 | 0.91 | 296 | 1.34 | 2 |
|  | SE05-1 | 188 | 0.72 | 232 | 4.76 | 1 |
|  | SE05-2 | 366 | 1.24 | 369 | 2.20 | 2 |
|  | SE05-3 | 413 | 1.34 | 419 | 1.49 | 3 |
|  | SE05-4 | 180 | 1.16 | 186 | 1.39 | 3 |
| Filled with normal concrete | CF05-1 | 877 | 1.57 | 927 | 2.98 | 4 |
|  | CF05-2 | 396 | 1.14 | 430 | 2.32 | 4 |
|  | CF05-3 | 550 | 0.97 | 607 | 2.72 | 4 |
|  | CF05-4 | 884 | 2.01 | 901 | 3.27 | 4 |
|  | SF05-1 | 301 | 0.89 | 306 | 1.22 | 6 |
|  | SF05-2 | 634 | 1.30 | 641 | 1.58 | 6 |
|  | SF05-3 | 878 | 1.60 | 892 | 1.89 | 6 |
|  | SF05-4 | 717 | 1.55 | 727 | 1.93 | 6 |
| Filled with polymer cement concrete | CP25-1 | 650 | 0.98 | 683 | 1.91 | 5 |
|  | CP25-2 | 277 | 0.93 | 295 | 5.79 | 5 |
|  | CP25-3 | 376 | 1.20 | 427 | 4.74 | 5 |
|  | CP25-4 | 638 | 1.56 | 656 | 2.13 | 4 |
|  | SP25-1 | 248 | 0.85 | 263 | 1.84 | 5 |
|  | SP25-2 | 518 | 1.02 | 531 | 1.54 | 6 |
|  | SP25-3 | 709 | 1.38 | 727 | 1.98 | 2 |
|  | SP25-4 | 551 | 1.33 | 565 | 1.90 | 6 |

voltage differential transducers (LVDT's) set on the corners of the specimens. No stress relief was carried out to eliminate the residual stresses in the steel tubes due to welding or cold forming.

## 3. Experimental results

Table 4 shows the yield load, yield displacement, maximum load, maximum displacement and failure mode for each of the test specimens. The yield load ($P_y$) is taken at the intersection point between the initial tangential line at the origin point and a tangential line with 1/3 the slope of the initial tangential line. Fig. 2 depicts the relationship between load and displacement for both the unfilled specimens and the concrete filled specimens.

### 3.1. Failure modes

Fig. 3 shows the generalized failure modes that were observed. The failure modes vary with respect to the shape of the steel tube, type of concrete, and width-thickness ratio. The failure modes can be described as follows:

(a) CF(P)-1

(b) CF(P)-2

(c) CF(P)-3

(d) CF(P)-4
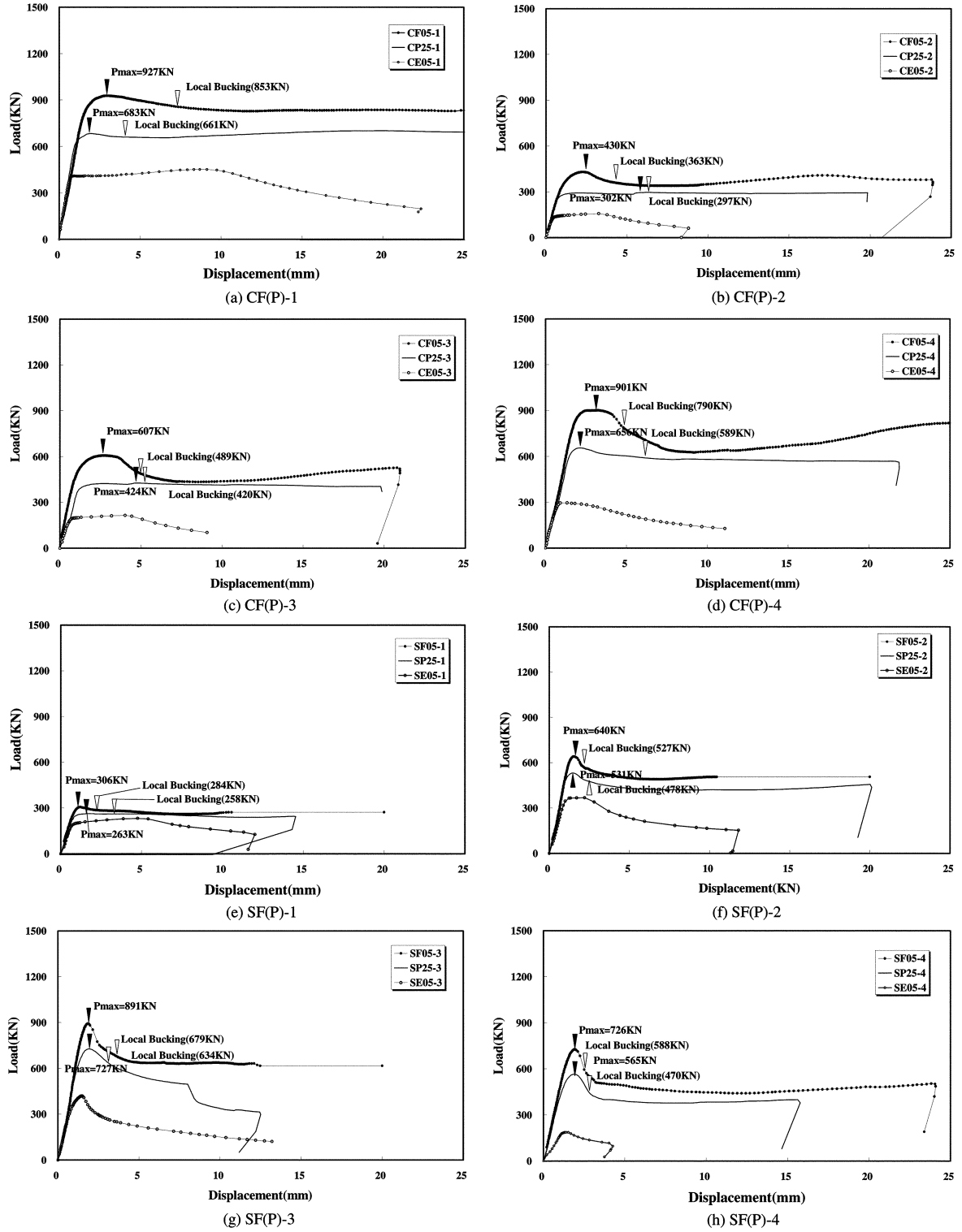
(e) SF(P)-1

(f) SF(P)-2

(g) SF(P)-3

(h) SF(P)-4

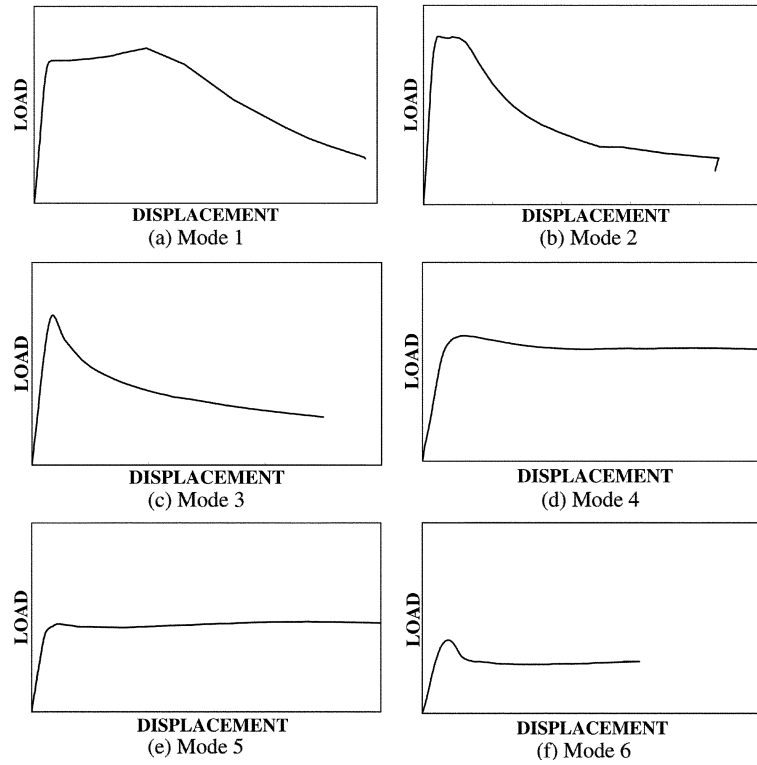Fig. 2 Relationship between load and displacement

Fig. 3 Failure modes

- Mode 1: load resistance initially increasing after yielding, and then gradually decreasing.
- Mode 2: load resistance gradually reducing after yielding.
- Mode 3: load resistance rapidly reducing after yielding.
- Mode 4: load resistance approximately constant after yielding.
- Mode 5: load resistance gradually increasing after yielding.
- Mode 6: load resistance initially decreasing after yielding, and the remaining approximately constant.

The hollow specimens exhibit failure modes 1, 2, and 3. Generally, the specimens with a lower *D/t* ratio exhibit failure mode 1, and as the *D/t* ratio increases specimens exhibit failure modes 2 and 3.

In the case of the concrete filled specimens, the relationship between load and displacement varies depending on the kind of steel section shape and the types of concrete. For circular specimens, those filled with normal concrete exhibited failure mode 4, and those filled with PCC exhibited failure mode 5 with the exception of the specimen with the highest *D/t* ratio, which exhibited failure mode 4. All of the square section specimens filled with normal concrete and PCC followed failure mode 6, with the exception the PCC-filled specimen with the lowest *D/t* ratio, which followed failure mode 5. The tests clearly showed the influence of both the steel cross section and the type of concrete filling on the behavior of stub columns, generally indicating that concrete-filled specimens exhibit a more ductile response than unfilled columns.
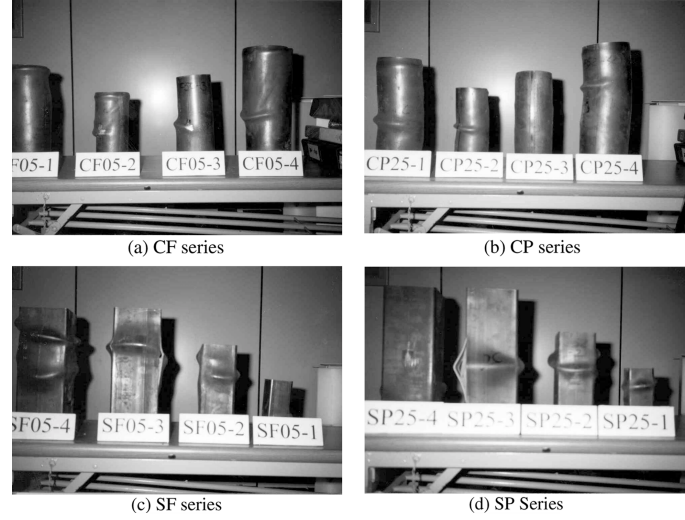
(a) CF series


(b) CP series


(c) SF series


(d) SP Series

Fig. 4 Specimens after testing

Table 5 Comparison of the filled with concrete specimens and hollow specimens

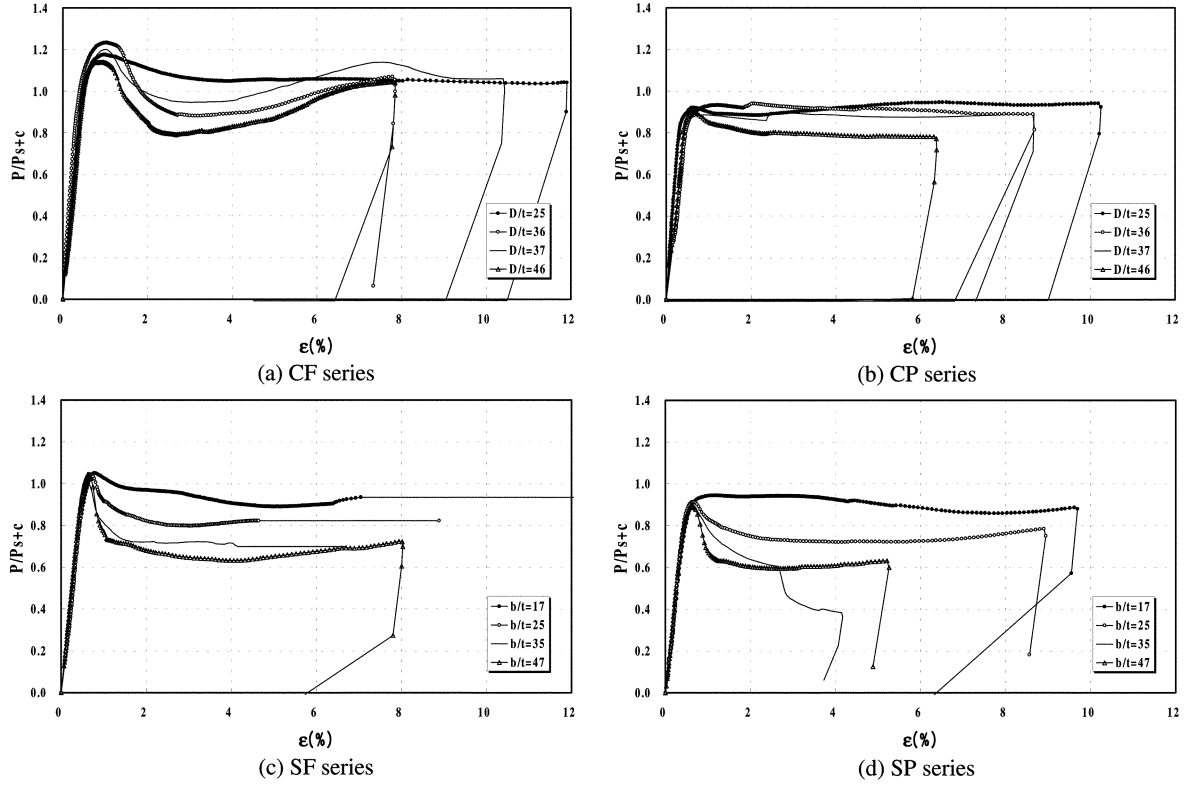| Specimen type | Diameter to thickness ratio | $P_{max}$ (KN) | $\dfrac{P_{F\_max}}{P_{H\_max}}$ | $\dfrac{\delta_{F\_max}}{\delta_{H\_max}}$ | $\dfrac{K_{F\_i}}{K_{H\_i}}$ | $P_{s+c}$ (KN) | $\dfrac{P_{max}}{P_{s+c}}$ |
|---|---|---|---|---|---|---|---|
| CE05-1 | | 463 | - | - | - | - | - |
| CF05-1 | 27 | 927 | 2.00 | 0.36 | 1.43 | 790 | 1.17 |
| CP25-1 | | 683 | 1.48 | 0.23 | 1.76 | 742 | 0.92 |
| CE05-2 | | 157 | - | - | - | - | - |
| CF05-2 | 37 | 430 | 2.75 | 0.71 | 2.56 | 358 | 1.20 |
| CP25-2 | | 295 | 1.89 | 1.78 | 2.19 | 330 | 0.89 |
| CE05-3 | | 215 | - | - | - | - | - |
| CF05-3 | 36 | 607 | 2.82 | 0.68 | 3.48 | 492 | 1.23 |
| CP25-3 | | 427 | 1.99 | 1.18 | 1.92 | 454 | 0.94 |
| CE05-4 | | 296 | - | - | - | - | - |
| CF05-4 | 46 | 901 | 3.05 | 2.44 | 1.48 | 791 | 1.14 |
| CP25-4 | | 656 | 2.22 | 1.59 | 1.38 | 727 | 0.90 |
| SE05-1 | | 232 | - | - | - | - | - |
| SF05-1 | 13 | 306 | 1.32 | 0.26 | 1.30 | 291 | 1.05 |
| SP25-1 | | 263 | 1.13 | 0.39 | 1.12 | 278 | 0.95 |
| SE05-2 | | 369 | - | - | - | - | - |
| SF05-2 | 22 | 641 | 1.74 | 0.72 | 1.67 | 614 | 1.04 |
| SP25-2 | | 531 | 1.44 | 0.70 | 1.73 | 581 | 0.91 |
| SE05-3 | | 419 | - | - | - | - | - |
| SF05-3 | 31 | 892 | 2.13 | 1.27 | 1.78 | 882 | 1.01 |
| SP25-3 | | 727 | 1.73 | 1.33 | 1.67 | 821 | 0.89 |
| SE05-4 | | 186 | - | - | - | - | - |
| SF05-4 | 43 | 727 | 3.90 | 1.39 | 2.29 | 696 | 1.04 |
| SP25-4 | | 565 | 3.03 | 1.37 | 2.05 | 633 | 0.89 |

Fig. 5 Relation between non-dimensional load and strain

## 3.2. Comparison of results for concrete-filled and hollow specimens

Table 5 shows the data for maximum load ratio, displacement ratio and initial stiffness ratio between hollow and filled specimens. The last column of Table 5 contains the maximum load ratios between the experimental data and the calculated results. It is observed that the ultimate strength of CFT stub columns filled with PCC is lower than the value of $P_{s+c}$. This is attributed to the difference in "composite action" between the two kinds of concrete fill used in the columns.

By comparing the maximum load ratios, it is observed that the normal concrete filling is generally more effective than the PCC for increasing the overall strength of the column. Fig. 5 shows the relationship between non-dimensional load and axial strain. Axial strain is obtained by dividing the measured axial displacement by the non-deformed length of specimen. Circular specimens filled with PCC exhibit stable behavior, where the load ratios do not decrease as the strain increases. Fig. 6 shows the maximum load ratio, initial stiffness, and non-dimensional load ratio as a function of the width to thickness ratio. The specimens are divided into four groups according to the type of concrete and shape of the cross section.

## 3.3. Load-axial strain response

The horizontal and vertical strains at the maximum load are listed in Table 6. The vertical strain ratio is in the range of 0.23 to 3.24 for the circular specimens and 0.13 to 2.74 for the square specimens. Fig. 7 depicts the relationship between the non-dimensional vertical and horizontal strains for the
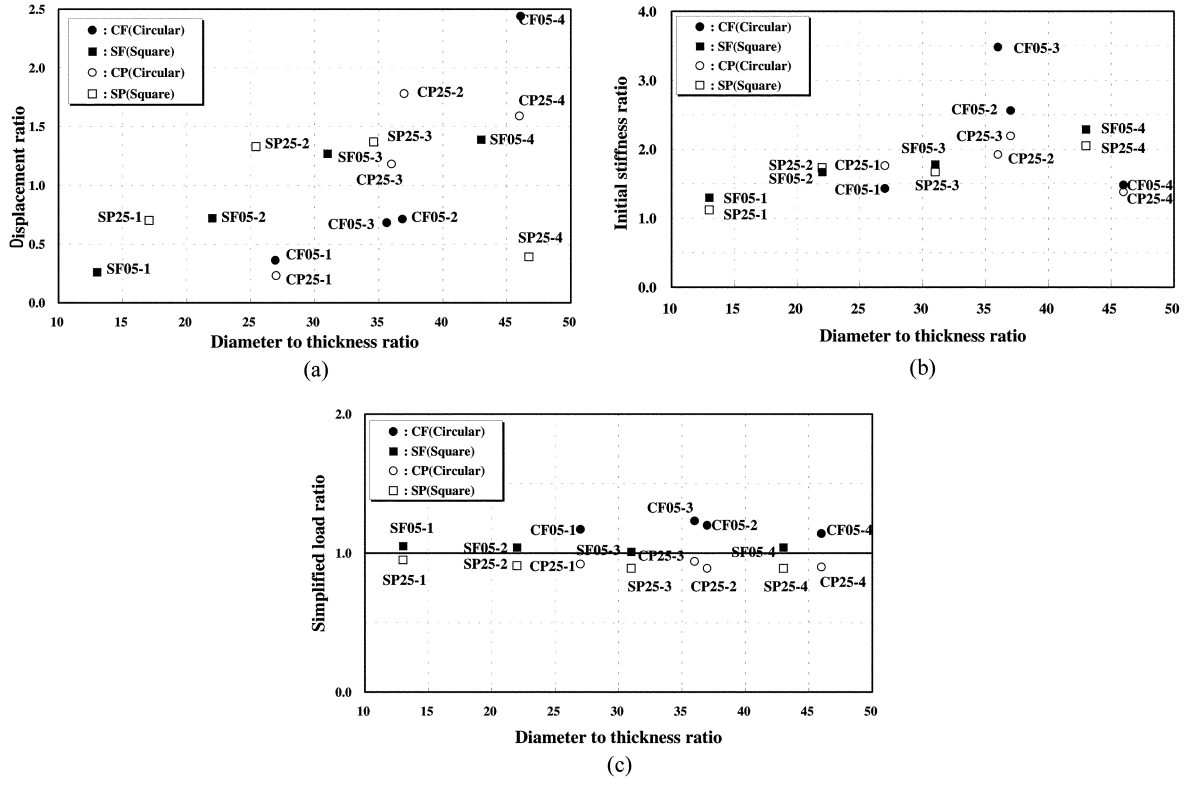
(a)

(b)

(c)

Fig. 6 Relationship between filling effect and diameter to thickness ratio



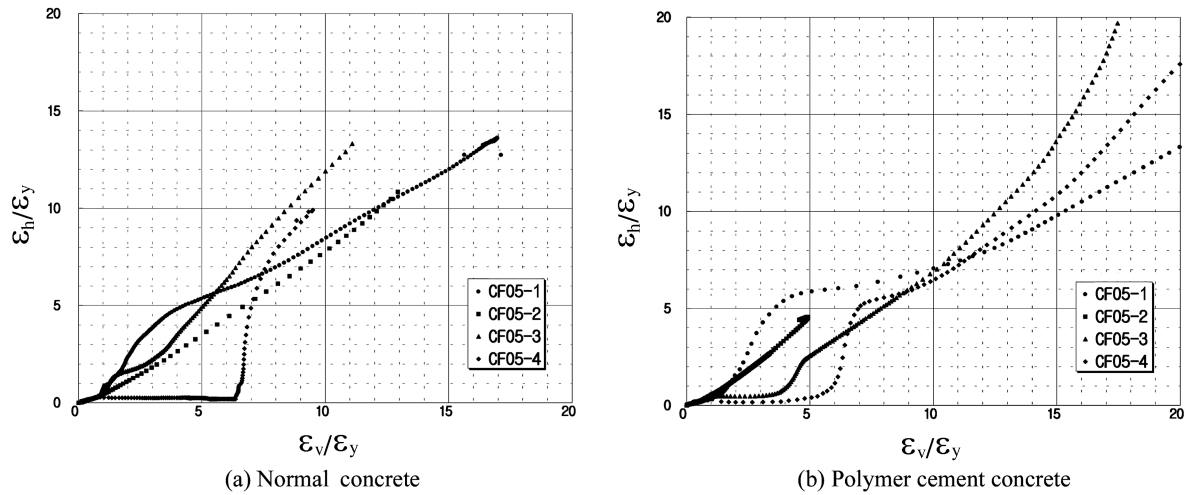(a) Normal concrete

(b) Polymer cement concrete
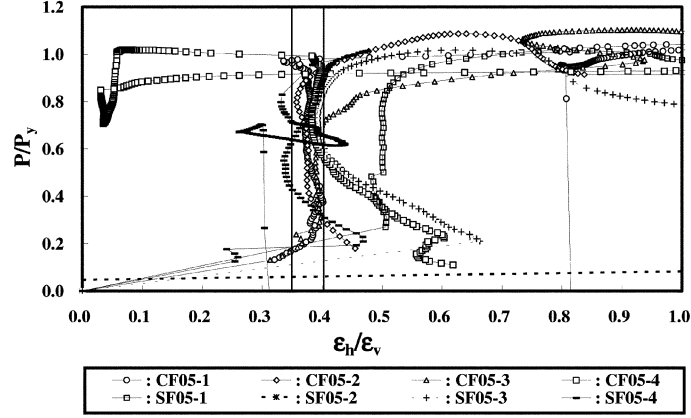
Fig. 7 Non-dimensional strains of circular section specimens

Table 6 Relationship between vertical and horizontal strain

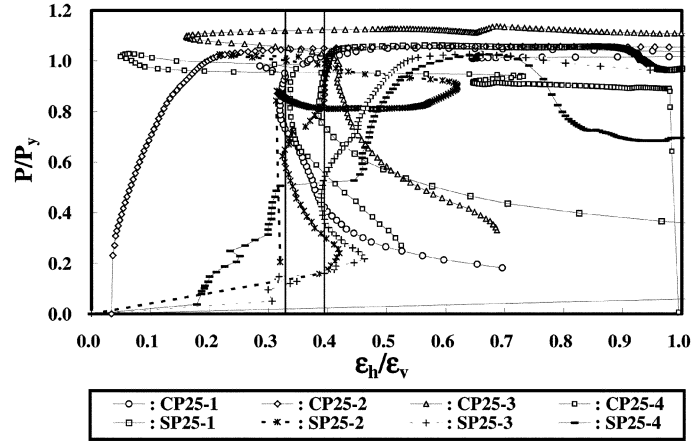| Specimen type | Diameter to thickness ratio | $\varepsilon_v$ ($\times 10^{-6}$) | $\varepsilon_h$ ($\times 10^{-6}$) | $\dfrac{\varepsilon_v}{\varepsilon_h}$ | $\dfrac{_f\varepsilon_v}{_h\varepsilon_v}$ |
|---|---|---|---|---|---|
| CE05-1 |    | -22034 | 9892  | 0.74 | -    |
| CF05-1 | 27 | -5114  | 6620  | 1.29 | 0.23 |
| CP25-1 |    | -68272 | 45923 | 0.67 | 3.10 |
| CE05-2 |    | -10237 | 5230  | 0.50 | -    |
| CF05-2 | 37 | -11967 | 7502  | 0.63 | 1.17 |
| CP25-2 |    | -13195 | 10983 | 0.83 | 1.29 |
| CE05-3 |    | -9914  | 4600  | 0.55 | -    |
| CF05-3 | 36 | -7618  | 6978  | 0.92 | 0.77 |
| CP25-3 |    | -9073  | 4702  | 0.52 | 0.92 |
| CE05-4 |    | -2628  | 628   | 0.23 | -    |
| CF05-4 | 46 | -8523  | 586   | 0.07 | 3.24 |
| CP25-4 |    | -6140  | 387   | 0.06 | 2.34 |
| SE05-1 |    | -23047 | 14996 | 0.65 | -    |
| SF05-1 | 13 | -3061  | 2513  | 0.82 | 0.13 |
| SP25-1 |    | -3089  | 1794  | 0.58 | 0.13 |
| SE05-2 |    | -3089  | 693   | 0.20 | -    |
| SF05-2 | 22 | -594   | 2379  | 4.01 | 0.19 |
| SP25-2 |    | -8484  | 1844  | 0.22 | 2.74 |
| SE05-3 |    | -3108  | 1760  | 0.57 | -    |
| SF05-3 | 31 | -3395  | 2111  | 0.62 | 1.84 |
| SP25-3 |    | -5111  | 3271  | 0.64 | 1.98 |
| SE05-4 |    | -1474  | 857   | 0.27 | -    |
| SF05-4 | 43 | -2711  | 1290  | 0.48 | 1.84 |
| SP25-4 |    | -2916  | 1963  | 0.67 | 1.98 |

circular section specimens. Strain data was obtained by wire strain gauges attached to the tube wall. Negative values denote compressive strains. Fig. 8 shows the relationship between the non-dimensional load and strain ratio. It is observed that the horizontal strain of PCC specimens is smaller than that of the specimens filled with normal concrete.

## 4. Comparison of experimental and calculated results

The calculated section capacities using the different codes are compared with test results for the circular and square section specimens in Table 7. The AISC design code strength for a CFT column subjected to concentrically compressive load is obtained by multiplying the nominal strength ($P_n$) by a resistance factor of 0.85.

(a) Normal concrete



(b) Polymer cement concrete

Fig. 8 Non-dimensional load and strain ratio

$$P_n = A_s F_{cr} \tag{1}$$

$$P_n = A_s F_{cr} \tag{2}$$

when $\lambda_c \leq 1.5$,
$$F_{cr} = (0.658\lambda_c^2) F_{my} \tag{3}$$

when $\lambda_c > 1.5$,
$$F_{cr} = \left[ \frac{0.877}{\lambda_c^2} \right] F_{my} \tag{4}$$

where
$$\lambda_c = \frac{Kl}{r_m \pi} \sqrt{\frac{F_{my}}{E_m}} \tag{5}$$

$$F_{my} = F_y + 0.85 f_c (A_c / A_s) \tag{6}$$

$$E_m = E + 0.4 E_c (A_c / A_s) \tag{7}$$

Table 7 Comparison of test and calculated results

| Specimen type | | $P_y$ (KN) | Calculated values | | | | Ratio | | | |
|---|---|---|---|---|---|---|---|---|---|---|
| | | | $P_{KSSC}$ (KN) | $P_{LRFD}$ (KN) | $P_{CISC}$ (KN) | $P_{EC4}$ (KN) | $P_y/P_{KSSC}$ | $P_y/P_{LRFD}$ | $P_y/P_{CISC}$ | $P_y/P_{EC4}$ |
| Normal concrete | CF05-1 | 877 | 715 | 664 | 631 | 790 | 1.22 | 1.34 | 1.39 | 1.15 |
| | CF05-2 | 396 | 302 | 299 | 284 | 358 | 1.31 | 1.22 | 1.39 | 1.14 |
| | CF05-3 | 550 | 416 | 412 | 391 | 493 | 1.32 | 1.36 | 1.41 | 1.15 |
| | CF05-4 | 884 | 704 | 688 | 660 | 791 | 1.26 | 1.29 | 1.34 | 1.09 |
| | SF05-1 | 296 | 234 | 250 | 322 | 291 | 1.29 | 1.25 | 0.94 | 1.09 |
| | SF05-2 | 637 | 468 | 506 | 478 | 614 | 1.36 | 1.17 | 1.33 | 1.12 |
| | SF05-3 | 584 | 661 | 741 | 701 | 882 | 1.33 | 1.13 | 1.25 | 1.03 |
| | SF05-3 | 584 | 661 | 741 | 701 | 882 | 1.33 | 1.13 | 1.25 | 1.03 |
| | Mean value | | | | | | 1.31 | 1.24 | 1.28 | 1.10 |
| | COV(coefficient of variation) | | | | | | 0.035 | 0.063 | 0.113 | 0.049 |
| Polymer cement concrete | CP25-1 | 650 | 674 | 602 | 592 | 742 | 0.91 | 1.06 | 1.10 | 0.92 |
| | CP25-2 | 277 | 278 | 268 | 261 | 330 | 1.00 | 1.05 | 1.06 | 0.86 |
| | CP25-3 | 376 | 383 | 377 | 360 | 454 | 0.98 | 1.05 | 1.05 | 0.85 |
| | CP25-4 | 638 | 649 | 611 | 607 | 727 | 0.98 | 1.05 | 1.05 | 0.86 |
| | SP25-1 | 248 | 226 | 225 | 311 | 278 | 1.09 | 1.12 | 0.80 | 0.95 |
| | SP25-2 | 518 | 448 | 458 | 451 | 582 | 1.16 | 1.13 | 1.15 | 0.97 |
| | SP25-3 | 709 | 624 | 664 | 651 | 821 | 1.14 | 1.07 | 1.09 | 0.90 |
| | SP25-4 | 551 | 491 | 546 | 534 | 633 | 1.12 | 1.02 | 1.03 | 0.84 |
| | Mean value | | | | | | 1.07 | 1.05 | 1.06 | 0.90 |
| | COV(coefficient of variation) | | | | | | 0.073 | 0.040 | 0.094 | 0.050 |

The Korean publication "Recommendations for the Design and Construction of Concrete Filled Tubular Structure" gives the following design equations for stub columns:

when $\dfrac{KL}{r_m} \leq C_c$

$$F_c = \frac{\left[1 - \dfrac{1}{2}\left(\dfrac{KL}{r_m C_c}\right)^2\right] F_{my}}{\dfrac{5}{3} + \dfrac{3}{8}\left(\dfrac{KL}{r_m C_c}\right) - \dfrac{1}{8}\left(\dfrac{KL}{r_m C_c}\right)} \tag{8}$$

when $\dfrac{KL}{r_m} > C_c$

$$F_c = \frac{12\pi^2 E_m}{23\left(\dfrac{KL}{r_m}\right)^2} \tag{9}$$

where

$$C_c = \pi\sqrt{\frac{2E_m}{F_{my}}} : \text{allowable compressive strength of long term load} \tag{10}$$

$$F_{my} = F_y + 0.6f_c(A_c/A_s) \quad \text{for square hollow section members} \tag{11}$$

$$F_{my} = F_y + \left(1 + 1.8\frac{t}{D}\frac{F_y}{f_c}\right)0.6f_{ck}(A_c/A_s) \quad \text{for circular hollow section members} \tag{12}$$

$$E_m = E_s + 0.4 E_c A_c \tag{13}$$

The Canadian Institute of Steel Construction gives the following equations for CFT stub columns subjected to concentrically compressive load. The limitations of the width-thickness ratios are given by

$$b/t \leq 1350/\sqrt{F_y} \qquad \text{for rectangular sections} \tag{14}$$

$$D/t \leq 28000/F_y \qquad \text{for circular sections} \tag{15}$$

The compressive resistance of the column is then calculated by

$$C_{rc} = \tau C_r + \tau' C_r' \tag{16}$$

where
$$C_r' = 0.85 \phi_c f_c' A_c \lambda_c^{-2} \left\lfloor \sqrt{1 + 0.25 \lambda_c^{-4}} - 0.5 \lambda_c^{-2} \right\rfloor \tag{17}$$

$$\lambda_c = \frac{KL}{r_c} \sqrt{\frac{f_c'}{\pi^2 E_c}} \tag{18}$$

$r_c$ is the radius of gyration of the concrete area, and $E_c$ is the initial elastic modulus for concrete, considering the effects of long-term loading.

For normal-weight concrete, with $f_c'$ expressed in MPa, this may be taken as $(1 + S/T) 2500 \sqrt{f_c'}$, where $S$ is the short-term load and $T$ is the total load on the column. For all rectangular hollow structural sections and circular hollow sections with a height-to-diameter ratio of 25 or greater, $\tau = \tau' = 1.0$, else

$$\tau = \frac{1}{\sqrt{1 + \rho + \rho^2}} \tag{19}$$

$$\tau' = 1 + \left(\frac{25\rho^2 \tau}{(D/t)}\right)\left(\frac{F_y}{0.85 f_c'}\right) \tag{20}$$

where
$$\rho = 0.02(25 - L/D) \tag{21}$$

The factor 0.85 is omitted for the filled tubes. This is due to the confining effect of the tube, which is considered in Eurocode4 ENV 1994-1-1:
For square sections, $P_{EC4} = A_s f_y + A_c f_c'$ \hfill (22)

For circular sections, $P_{EC4} = \eta_2 A_2 f_y + [1 + \eta_1(t/d)(f_y/f_c')] A_c f_c'$ \hfill (23)

where
$$\eta_1 = \eta_{10}(1 - 10e/d) \qquad \eta_{10} = 4.9 - 18.5\bar{\lambda} + 17\bar{\lambda}^2$$

$$\eta_2 = \eta_{20} + (1 - \eta_{20})(10e/d) \qquad \eta_{20} = 0.25(3 + 2\bar{\lambda})$$

$$\bar{\lambda} = \sqrt{N_{plR}/N_{cr}}, \leq 0.2 \qquad N_{cr} = \pi^2 (EI)_c/l^2, (EI)_c = E_s I_s + 0.6 E_{cm} I_c$$

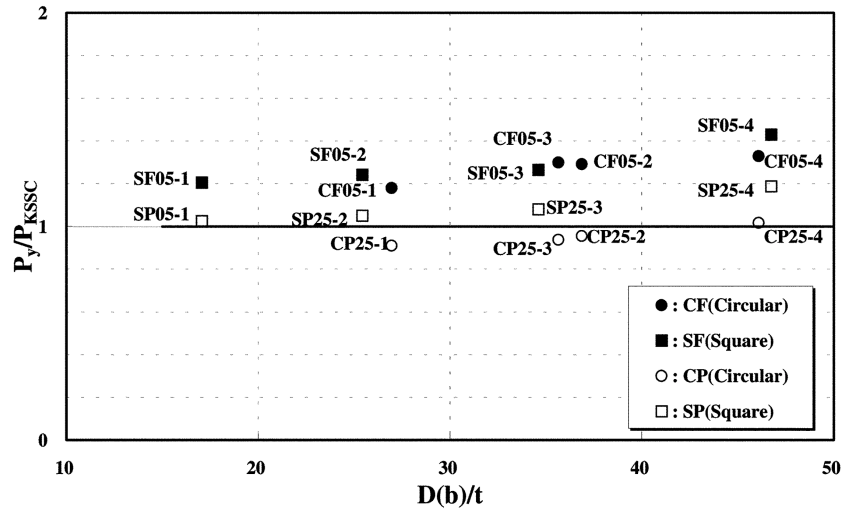$$E_{cm} = 9.5(f_c' + 8)^{1/3}$$

Fig. 9 Relationship between load ratio (KSSC) and diameter (width) to thickness ratio
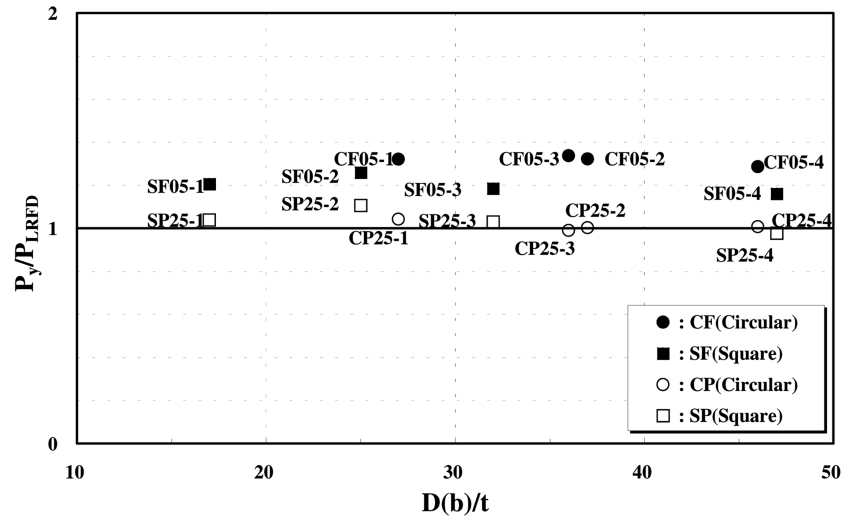


Fig. 10 Relationship between load ratio (LRFD) and diameter (width) to thickness ratio

The calculated values in the table were obtained by adapting the code formulations without resistance factors. For normal concrete, the average ratios of test results to calculated ones were 1.27 and 1.19 for circular and square sections, respectively. For PCC, the average ratios were 0.99 and 1.03 for circular and square sections, respectively. As shown in Table 7, the method proposed by AISC-LRFD and EC4 give a mean of 1.24 and 1.10, a COV of 0.063 and 0.049 for the stub columns filled with normal concrete, respectively. For PCC, the method proposed by AISC-LRFD and EC4 give a mean of 1.05 and 0.90, a COV of 0.040 and 0.050 for the specimens filled with polymer cement concrete, respectively. Fig. 9 to Fig. 12 respectively represent the relationship between the ratios of test data to calculated values and diameter to thickness ratios.
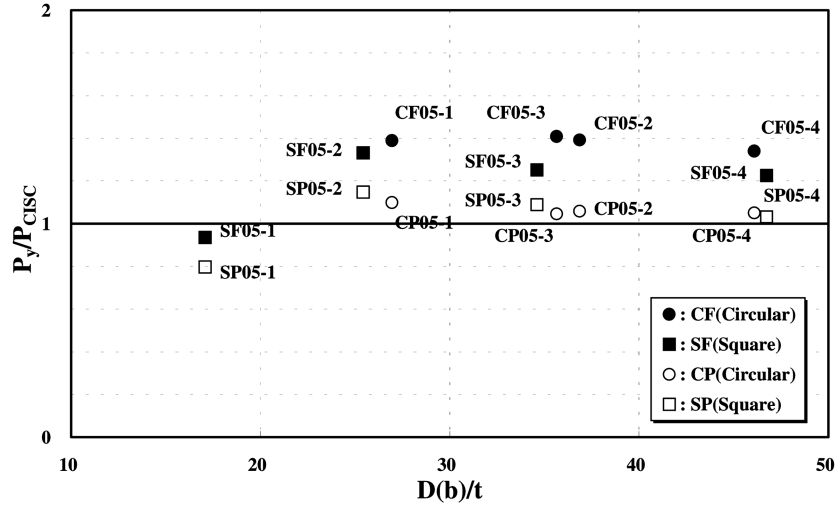
Fig. 11 Relationship between load ratio (CISC) and diameter (width) to thickness ratio
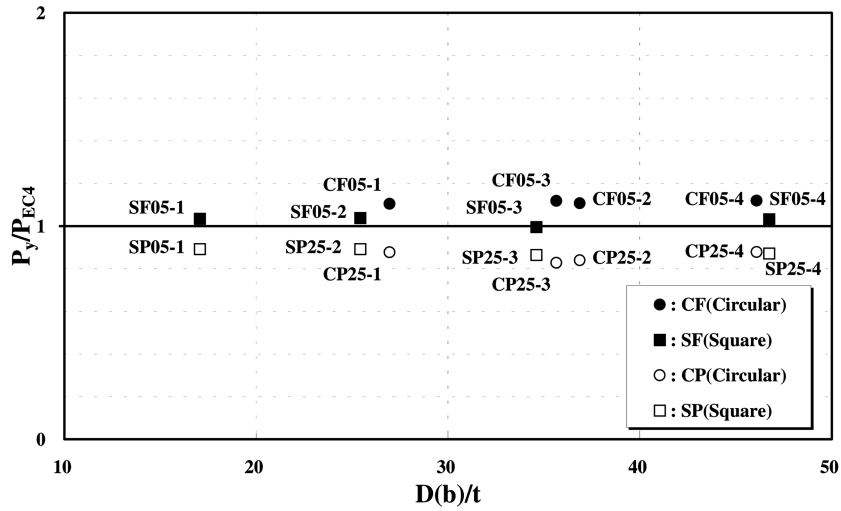


Fig. 12 Relationship between load ratio (EC4) and diameter (width) to thickness ratio

## 5. Conclusions

Experimental results have shown that the behavior of steel stub columns with respect to their type of filling can be described as follows:

1. The performance of the circular section specimens filled with concrete was compared with the hollow section specimens. For normal concrete fill, the ratio of filled to hollow results varied from 2.00 to 3.05 (mean value 2.67) for maximum load resistance, 0.36 to 2.44 (mean value 1.05) for the maximum displacement, and 1.43 to 3.48 (mean value 2.24) for the initial stiffness. For PCC fill (CP series), the ratio of filled to hollow results varied from 1.48 to 2.22 for maximum load resistance, 0.23 to 1.78 for the maximum displacement, and 1.38 to 2.19 for the initial stiffness.

2. Certain maximum displacement ratios as mentioned above were less than 1.0. This was attributed to different failure modes that occur due to the diameter to thickness ratio of steel tubes.

3. For circular specimens, the average value of the ratio of filled to hollow maximum strain was 1.35 for normal concrete fill, and 1.91 for PCC fill.

4. Test results for compressive resistance were compared with values calculated using KSSC, AISC-LRFD, CISC, and EC4 codes. It was observed that in general the ratio of test results to calculated results is lower for PCC than for normal concrete.

5. For normal concrete, the average ratios of test results to calculated ones were 1.27 and 1.19 for circular and square sections, respectively. For PCC, the average ratios were 0.99 and 1.03 for circular and square sections, respectively.

6. Circular steel tube specimens filled with high strength polymer concrete did not show a sudden decline in load-carrying capacity beyond ultimate load.

## Acknowledgements

## References

American Institute of Steel Construction (1994), *Load and Resistance Factor Design*, Volume I, 2nd edition, American Institute of Steel Construction, Inc, Chicago.

Bradford, M.A., Loh, H.Y. and Uy, B. (2002), "Slenderness limits for filled circular steel tubes", *J. Constructional Steel Research*, **58**, 243-252.

British Standards Institution (1994), Eurocode 4, *Design of Composite Steel and Concrete Structures, Part 1.1: General Rules and Rules for Buildings* DD-ENV 1994-1-1, London.

Campione, G. and Scibilia, N. (2002), "Beam-column behavior of concrete filled steel tubes", *Steel and Composite Structures*, **2**(4), 259-276.

Campione, G., Mindness, S., Scibilia, N. and Zingone, G. (2000), "Strength of hollow circular steel sections filled with fiber-reinforced concrete", *Canadian J. Civil Eng.*, **27**, 364-372.

Canadian Institute of Steel Construction (1997), *Handbook of Steel Construction,* 7th edition, ISBN 0-88811-088-X, Ontario.

Dunberry, E., Leblanc, D. and Redwood, R.G. (1987), "Cross-section strength of concrete-filled HSS columns at simple beam connections", *Canadian J. Civil Eng.*, **14**, 408-417.

Elremaily, A. and Azizinamini, A. (2002), "Behavior and strength of circular concrete-filled tube columns", *J. Constructional Steel Research*, **58**, 1567-1591.

Furlong, R.W. (1968), "Design of steel-encased concrete beam-columns", *J. Struct. Div.*, ASCE **94**(ST1), 267-281.

Hajjar, J. F. and Gourley, B. C. (1996), "Representation of concrete-filled steel tube cross-section strength", *J. Struct. Eng.,* **122**(11), 1327-1336.

Han, Lin-Hai, Yao, Guo-Huang, and Zhao, Xiao-Ling (2004), "Behavior and calculation on concrete-filled steel CHS (circular hollow section) beam-columns", *Steel and Composite Structures*, **4**(3), 787-804.

Han, Lin-Hai, (2002), "Test on stub columns of concrete-filled RHS sections", *J. Constructional Steel Research*, **58**(3), 353-372.

Han, Lin-Hai, Tang, You-Fu, and Xu, Lei (2003), "An experimental study and calculation on the fire resistance of concrete-filled SHS and RHS columns", *J. Constructional Steel Research*, **59**, 427-452.

Huang, C.S., Yeh, Y.K., Liu, G.Y., Hu, H.T., Tsai, K.C., Weng, Y.T., Wang, S.H. and Wu, M.H. (2002), "Axial load behavior of stiffened concrete-filled steel columns", *J. Struct. Eng.*, ASCE, **128**(9), 1222-1230.

Knowles, R.B. and Park, R. (1969), "Strength of concrete filled steel tubular columns", *J. Struct. Div.,* ASCE **95**(ST12), 2565-2587.

Korean Society of Steel Construction (2001), *Recommendations for the Design and Construction of Concrete Filled Tubular Structures,* 1st edition, Seoul.

Picard, A. and Beaulieu, D. (1997), "Resistance of concrete-filled hollow structural sections", *Canadian J. Civil Engineering*, **24**, 785-789.

Prion, H.H.L. and Baraka, M. (1994), "Thin-walled tubes filled with high strength concrete", *Canadian J. Civil Eng.*, **21**(1), 207-218.

Schneider, S. P. (1998), "Axially loaded concrete-filled steel tubes", *J. Struct. Eng.*, **124**(10), 1125-1138.

## Notation

| | |
|---|---|
| $A_c$ | : cross-sectional area of concrete |
| $A_s$ | : cross-sectional area of steel tube |
| $C_c$ | : allowable compressive strength |
| $C_{rc}$ | : factored compressive resistance of a composite column |
| $C_r$ | : factored compressive resistance of a steel member |
| $C_r{}'$ | : factored compressive resistance of a concrete eel member |
| $E_m$ | : modified modulus of elasticity for the design of composite column |
| $E_c$ | : elastic modulus of concrete |
| $E_s$ | : elastic modulus of steel |
| $F_{cr}$ | : critical stress |
| $F_{my}$ | : modified yield stress for the design of composite column |
| $Kl$ | : effective buckling length |
| $K_{F\_i}/K_{H\_i}$ | : initial stiffness ratio between infilled and hollow stub column |
| $P_{F\_max}/P_{H\_max}$ | : load ratio between infilled and hollow stub column |
| $P_{max}$ | : measured maximum load |
| $P_n$ | : nominal axial strength |
| $P_y$ | : measured yield load |
| $S$ | : short term load |
| $T$ | : total load of the column |
| $f_c'$ | : compressive strength of concrete cylinder |
| $r_m$ | : radius of gyration of steel pipe |
| $\delta_y$ | : measured yielding displacement corresponding $P_y$ |
| $\delta_{max}$ | : measured yielding displacement corresponding $P_{max}$ |
| $\delta_{F\_max}/\delta_{H\_max}$ | : displacement ratio between infilled and hollow stub column |
| $\varphi_c$ | : resistance factor |
| $\rho$ | : slenderness ratio |
| $CC$ | |